RESEARCH ARTICLE
doi: 10.2306/scienceasia1513-1874.2017.43.001

ScienceAsia 43 (2017): **1–7**

Microbially induced $CaCO_3$ precipitation: hydraulic response and micro-scale mechanism in porous media

Yefei Tan[a,*], **Xinghua Xie**[a], **Shiqiang Wu**[a], **Tao Wu**[b]

[a] Nanjing Hydraulic Research Institute, Nanjing, 210029, China
[b] Jiangsu Provincial Centre for Disease Control and Prevention, Nanjing, 210024, China

*Corresponding author, e-mail: tan8112@gmail.com

Received 21 Apr 2016
Accepted 7 Mar 2017

ABSTRACT: Microbially induced $CaCO_3$ precipitation (MICP) is a natural process which has recently been applied as a technique for soil solidification and hydraulic conductivity reduction. In the present study, laboratory-based MICP tests were carried out in four columns containing sand with different particle sizes together with cultures of *Sporosarcina pasteurii*. A calcium solution was supplied continuously to the columns at a speed of 0.97 ml/min to mimic underground seepage. Hydraulic conductivities in the columns were monitored by hydraulic tests before and during MICP. Results showed that the reduction in conductivity values could be as high as 97% after 24 h of MICP. Columns clogged with calcite precipitates were examined by environmental scanning electron microscopy and energy dispersive X-ray spectroscopy. Calcite precipitation was shown to be the reason for hydraulic conductivity reduction. The calcium precipitation rates and amounts were quantified and verified.

KEYWORDS: hydraulic conductivity reduction, calcium precipitation, MICP

INTRODUCTION

Unexpected underground percolation is a global concern from environmental and civil engineering perspectives. It can cause water pollution and vast losses in water resources. For example, millions of people worldwide depend on dams and reservoirs for energy, fresh water, and flood protection. Unfortunately, such dams, especially earth dams, are usually threatened by leakage[1]. Moreover, groundwater contamination due to leakage from landfills is increasingly becoming a worrying issue[2,3]. The traditional method to stop such leakage has been injection of cement or other chemical materials into the crack sites (e.g., fractures or holes in an earth dam or a landfill); however, this can easily cause secondary pollution.

Microbially induced $CaCO_3$ precipitation (MICP) is a common phenomenon widely found in nature. It has recently been used for purposes as diverse as permeability reduction and soil solidification by cementing soil particles together using a supply of calcium and urea[4,5]. A non-exhaustive list of papers provided in the literature in recent years shows that there has been a long-standing interest in the MICP technique using different ureolytic bacteria[6,7]. The most studied bacterium in this realm is *Sporosarcina pasteurii* (formerly known as *Bacillus pasteurii*), which has the highest urea-hydrolysing capability among all known bacteria[8,9]. Compared to other ureolytic bacteria like *B. sphaericus* (both ATCC 21776 and 21787), it also has advantages such as higher stability, better tolerance to high concentrations of ammonium, and more consistent urease production[10].

Calcite precipitation is a complex process, and bacterial metabolic activities play a key role in ureolysis and calcite precipitation reactions[11,12]. The reaction occurs as

$$CO(NH_2)_2 + 2H_2O \xrightarrow{\text{urea hydrolysis}} 2NH_3 + H_2CO_3$$
$$2NH_3 + H_2CO_3 + Ca^{2+} \xrightarrow[\text{precipitation}]{} 2NH_4{}^+ + CaCO_3.$$

Controlling this novel environment-friendly technology could benefit a variety of fields such as foundation reinforcement, permeability reduction, and pollutant removal[13,14]. However, MICP is a very complex process that depends on several factors like the saturation state of calcium ions, mobility of ions, and conductivity of porous media[15,16]. Simultaneously, MICP has an opposite impact on hydraulic conductivity by decreasing porosity, which affects ion transport and reduces conductivity[17]. Two major limitations to MICP in porous media have been suggested: first, the pore size of the medium

($> 0.5\,\mu$m), through which bacteria can move freely, and second, the need for the removal of residual products of MICP from the porous media or their conversion to neutral products such as water, CO_2, or nitrogen[18]. For decades, research groups have tried to apply this technology for permeability reduction[19,20]; however, the mechanisms and effects of MICP in porous media are unknown[17,21]. The objective of this study was to understand the micro-scale mechanisms of MICP and the response of hydraulic conductivities in different sand columns.

MATERIALS AND METHODS

Bacterial culture and enrichment

In this study, *S. pasteurii* (DSMZ-33; purchased from the DSMZ-German collection of microorganisms and cell cultures) was chosen as the ureolytic bacteria in the experiments. The culture medium was prepared according to DSMZ as follows: tryptone 15 g/l; soy peptone 5 g/l; NaCl 5 g/l and urea 20 g/l. To the medium (1 l), 15 g agar was added. The medium was then autoclaved at 121 °C for 20 min. The culture plates were incubated overnight at 32 °C, and the colonies were transferred into a 50-ml shaking flask with growth solution (based on the DSMZ recipe) and shaken for 15 h. Note that this bacterial suspension contained carbonate ions that were produced by the bacteria during the shaking. Thus the suspension could not be directly used for the columns until all the CO_3^{2-} had been removed. To remove the CO_3^{2-}, the bacteria were centrifuged at 10 000g for 10 min and rinsed twice with pure water (Milli-Q Academic A10, Millipore, USA). Then the bacteria were transferred into another flask to be kept as a bacterial stock for later use. The optical density of this bacterial stock was measured to be 2.32 (2.22×10^9 cells/ml) at 600 nm with a spectrophotometer. The MICP solution was prepared as follows[22]: tryptone 10 g/l; soy peptone 2 g/l; $CaCl_2$ 50 g/l and urea 30 g/l. This solution (pH 6.9; dissolved oxygen 26%) was autoclaved and cooled down to room temperature before use.

Table 1 Materials of sand columns.

No.	Average particle diameter (mm)	Packed weight (g)	Column porosity (%)
1	0.238	143.0	26.6
2	0.473	135.0	28.0
3	0.940	130.9	29.2
4	1.875	129.0	31.2

MICP and hydraulic tests for sand columns

Four types of silica sand (Table 1) were prepared for our tests (Fig. 1) and were packed in stainless steel cylinders (length 7.5 cm; inner diameter 3.5 cm). Sand was washed with HCl solution and rinsed with pure water to obtain rid of the interference of impurities before use. Two pebble filter layers were installed at both ends of the cylinders to curb

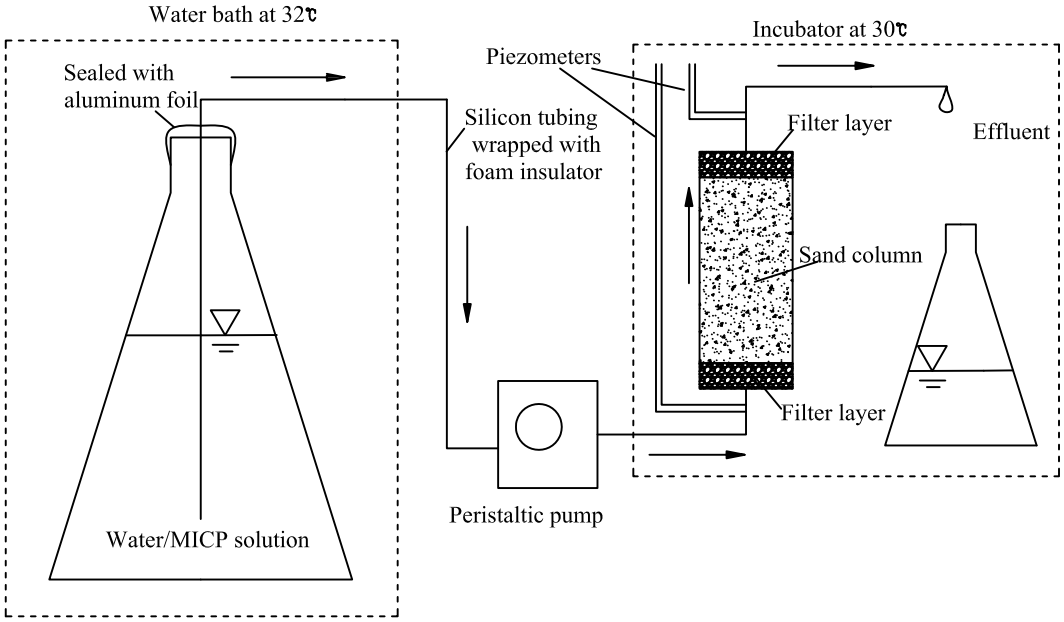

Fig. 1 Setup of MICP and hydraulic tests.

the movement of sand during the water flush. Two piezometers were used to monitor the water pressure at both ends of the column. Water/solution was pumped into the column from the bottom using a peristaltic pump to ensure that the whole column was saturated and the inner flow was steady. The cylinders were placed in an incubator at 30 °C, and the source solution was in a water bath at a constant temperature of 32 °C. The connecting silicone tubing was wrapped with a foam insulator to avoid heat loss. Prior to the test, the columns were flushed with 75% alcohol and then rinsed overnight with pure water at a speed of 2 ml/min to avoid contamination from other bacteria (Fig. 1).

Next, hydraulic tests were conducted at 3 different flow rates (0.56, 0.97, and 1.73 ml/min, corresponding to pumping rates of 1, 0.5, and 2 rpm) using pure water to obtain an average conductivity before MICP. Then, 20 ml of bacterial stock solution(approximately 4.44×10^{10} cells) was inoculated into each column with a pumping rate of 0.97 ml/min of pure water, and the effluent was collected for cell counting. About 10 pore-volumes later, the MICP solution was then pumped into the columns at a speed of 0.97 ml/min until the test was stopped 72 h later. Hydraulic tests were conducted every 12 h during the MICP test.

Environmental scanning electron microscopy and energy dispersive spectroscopy examination

Subsequently to the MICP test, the 4 MICP-treated column samples (which were clogged with precipitated calcite) were carefully dried, weighed (Shimadzu ATX124, Japan) and cut at room temperature. Crystals were examined by environmental scanning electron microscopy (ESEM, FEI Quanta 650 FEG, Environmental SEM) and its composition determined by energy dispersive X-ray spectroscopy (EDS) (INCA X-act Silicon Drift Detector, Oxford Instruments).

RESULTS

Bacteria absorption in columns

Assuming the number of bacterial cells was constant during the flushing, and then the number of bacterial cells adsorbed in each column can be obtained by subtracting cell number in the effluent with the inoculated number[3]. For each column the adsorbed numbers of cells were calculated as 2.15×10^9, 2.06×10^9, 1.97×10^9, and 1.61×10^9, respectively, for columns 1–4. This suggested that the columns packed with larger particles adsorbed/blocked fewer bacterial cells than those with smaller ones due to larger pore volumes and better connection between pores.

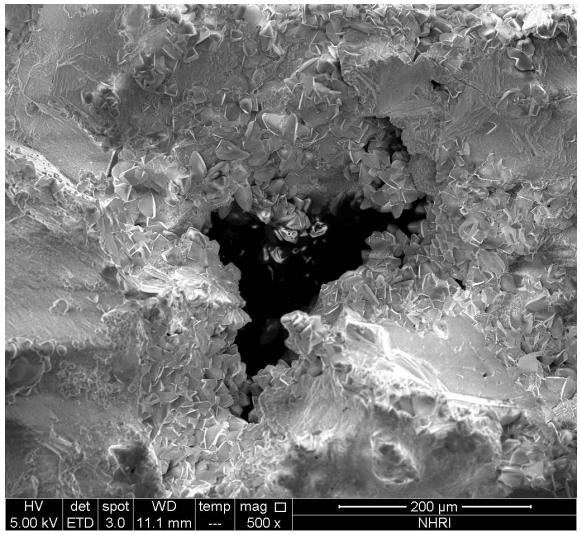

Fig. 2 Microbially induced calcite precipitation in pores between sand particles.

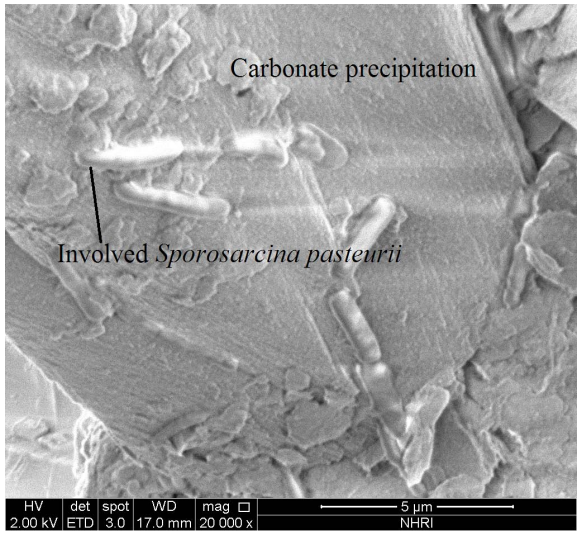

Fig. 3 Calcium precipitation with involved bacterial cells.

Environmental scanning electron microscopy and energy dispersive spectroscopy

The MICP-treated samples were examined by ESEM to observe the calcite clogging between sand particles (Fig. 2 and Fig. 3). It was expected that the calcite deposits exist mainly as separated crystals in the pores[12], however, they were found "to grow" and coated on the surfaces of sands. Since calcium ions

Table 2 Analysed elements and their oxide concentrations in crystals.

Elem	Oxides	Element concentration	Weight (%)	Atom (%)	Compound (%)
C	CO_2	13.15	11.16	18.93	40.88
Si	SiO_2	0.50	0.45	0.33	0.97
S	SO_3	0.43	0.37	0.24	0.94
Cl	Cl	0.44	0.44	0.25	0.00
Ca	CaO	45.47	39.36	20.01	55.07
Mn	MnO	1.16	1.32	0.49	1.70
O			46.90	59.74	

in the solution were attached to the bacterial cell wall due to the negative charge of the latter to form deposits, many cells were buried in the deposits and lost the capability of attracting ions. To continue the precipitation and consequently reduce the hydraulic conductivity to a lower level, bacterial reproduction which is controlled by nutrient transport system of the cells is essential. However, the capability of urea hydrolysis was becoming weaker and weaker due to the narrowing flow paths.

Next, an EDS equipped with an analytical silicon drift detector was used to analyse the crystal composition. In this detection, X-rays emitted from the sample atoms have a characteristic energy and wavelength; carbon, for example, has only 1 peak (a K alpha X-ray at 0.282 keV) while calcium has 3 peaks, based on the presence of the elements in the analysed sample can be confirmed. Moreover, the detected elements can also be quantified with a very low error. Oxide concentrations given in Table 2 suggest that the compound percentages of CaO and CO_2 were 55% and 41%, respectively. This indicates that calcite is the main compound of the precipitate ($>$ 95% in weight percentage). Except for calcite, the rest of the CaO exists in the form of wollastonite ($CaSiO_3$).

Hydraulic conductivity reduction

Hydraulic conductivity of porous media can be calculated according to Darcy's law,

$$K = \frac{q}{AJ},$$

where K is the conductivity (L/T); q is the flow rate (L^3/T), which could be controlled by the pump rate in our tests; A is the cross-sectional area of the column (L^2); and J is the dimensionless hydraulic gradient, which is a vector gradient between two hydraulic head measurements over the distance of the flow path,

$$J = \frac{\Delta h}{\Delta l},$$

where Δh is the difference between two hydraulic heads and Δl is the distance between the two points.

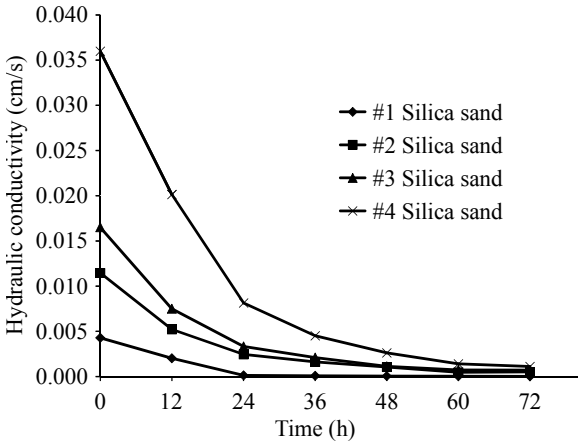

Fig. 4 Changes in hydraulic conductivities of columns over time.

The changes in the conductivity of each column are shown in Fig. 4. We observed that the values of conductivity decreased faster in the first 24 h than in the later period and then slowly became stable. This was expected because MICP has 2 prerequisites, namely, urea-hydrolysing microbes and calcium ions. Nutrients are essential for the bacteria to maintain a certain rate of urea hydrolysis, while calcium ions are the source for calcite crystals. Fluid flow acts as the vehicle for both nutrients and calcium transport and is therefore important for the MICP process. During the process of calcium precipitation, the pores in the column were gradually filled with calcite precipitates, which limited and/or cut off the inner flow paths and caused a lower conductivity. Consequently, the capacity of flow for nutrients and calcium ion transport decreased, causing slower precipitation. Among these columns, column 1, in particular, achieved hydraulic conductivity reductions of 97% from its initial value after 24 h of MICP. The remaining columns had reductions ranging from 77% to 89%.

The amount of calcium precipitate mainly depends on the inner active bacteria population, a larger quantity of bacteria has a greater capability of urea-hydrolysing to produce more calcium precipitate. However, (Fig. 4), though the columns packed with larger particle sizes had fewer bacteria absorbed in the beginning before MICP. They obtained faster calcium precipitation speed (Steeper

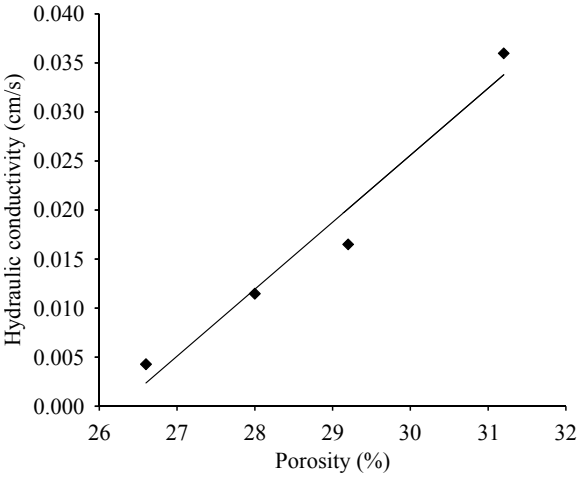

Fig. 5 Initial conductivity values of the 5 columns before MICP vis-à-vis porosity values; line: $y = 0.006\,x - 0.179$, $R^2 = 0.960$.

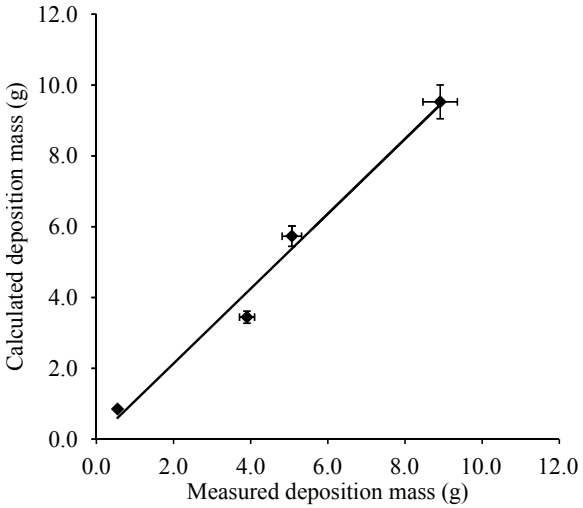

Fig. 6 Relation between calculated and measured calcium precipitation masses; line: $y = 1.0573\,x + 0.0185$, $R^2 = 0.9831$.

slope in Fig. 4) compared with columns with smaller pore sizes during a certain period. This implies that the small differences (all the 4 columns had the same order of magnitude of cell population) among the initial bacterial populations before MICP were not as important as nutrient transport for calcite precipitation.

$CaCO_3$ precipitation

The dry weights of each column increased 0.548 g, 3.902 g, 5.065 g, and 8.911 g for columns 1–4, respectively. As shown in Fig. 5, the calculated initial hydraulic conductivities were linearly related to the column porosities:

$$n = \frac{K + 0.1793}{0.0068},$$

where n is the porosity and K is the hydraulic conductivity. This relationship was expected because the column with a smaller porosity had narrower flow pathways between sand particles. Although it is difficult to exactly quantify the hydrolysed urea, we can estimate the deposited $CaCO_3$ by applying the linear relationship between porosity and hydraulic conductivity:

$$M_{Ca} = \left(n_0 - \frac{K_d + 0.1793}{0.0068} \right) V_{col}\, \rho_{Ca},$$

where M_{Ca} is the mass of $CaCO_3$ precipitation, n_0 denotes the initial porosity of the column, K_d denotes the hydraulic conductivity after MICP, V_{col} is the column volume, and ρ_{Ca} denotes the density of $CaCO_3$. The volume of the columns was calculated as 72.122 cm^3, and the density of $CaCO_3$ is 2.71 g/cm^3. Using this information we calculated the weight of precipitate in each column: 0.850 g, 3.446 g, 5.733 g, and 9.525 g, for columns 1–4, respectively. This was in agreement with our measured results (Fig. 6), and indicated that the amount/volume of calcium precipitate which was controlled by the capability of inner urea-hydrolysing had a direct impact on the hydraulic conductivity reduction rather than that of the initial bacterial cell.

The precipitation rate of $CaCO_3$ of *S. pasteurii* was suggested as $4.0 \pm 0.1 \times 10^{-6}$ g/cell according to previous studies[3]. However, the amount of precipitated $CaCO_3$ is much lower than that expected. One of the reasons for this could be the different ways of bacteria injection. Former researchers[3] injected bacteria under a stopped flow condition to achieve better adsorption while the continuous flow injection was adopted in our experiment to mimic the seepage in nature. These two ways of injection can affect the distribution of bacteria in the porous media. Besides, the flow paths were much more complex and torturous than those in Eryürük et al[3] whose columns were made of smooth glass beads. Thus the impacts from inner flow losses (e.g., frictional losses, losses due to eddy currents, losses due to bends) became significant and much more important than expected for calcium precipitation.

To quantify the relation between increased sand average diameter and hydraulic conductivity reduc-

tion, a modified Kozeny-Carman model was used[3]. This model was established based on the premise of deposits coated on sand particles rather than separated particles, which had been proved by our ESEM findings. This model can be written as follows.

$$K_{\mathrm{d}} = \frac{f\rho g(n - V_{\mathrm{Ca}}/V_{\mathrm{col}})^3(6V_{\mathrm{Ca}}/\pi + D^3)^{2/3}}{36\mu(1 - n + V_{\mathrm{Ca}}/V_{\mathrm{col}})^2},$$

where f is the shape factor obtained by fitting the initial measured hydraulic conductivities of columns before MICP, V_{Ca} is the volume of calcium deposits, ρ is the liquid density, g denotes gravity, μ is the dynamic viscosity of water, and D is the diameter of sand particles before and after MICP. Thus the increase in the particle size resulted in the decrease of hydraulic conductivity. The shape factors of each column were estimated as 0.89, 0.50, 0.15, and 0.07 for columns 1–4, respectively. The values of ρ, g, and μ were 1050 kg/m^3, 9.80 m/s^2 and 0.0117 kg/ms, respectively. Then, the rates of average diameter increase of each column after 72 h of MICP could be obtained as 3%, 16%, 16%, and 11%, respectively. This indicates that in columns packed with fine particles like column 1, precipitation is more difficult to occur compared with the other three columns.

DISCUSSION

In summary, MICP in 4 columns packed with different sized sand particles were studied under a constant flow rate. Hydraulic conductivity reduction was found to be much faster during the first 24 h and could cause a reduction as great as 98%. ESEM and EDS examination confirmed that $CaCO_3$ precipitation on sands was the cause for hydraulic conductivity reduction. Although larger pore sized columns adsorbed lesser bacteria at the beginning, they had faster precipitation speeds and more calcium deposits after a certain period. Thus a good nutrient transport network is crucial for MICP in porous media. Except for the bacteria injection method, the precipitation can also be largely affected by flow losses more than was expected.

This study enables us to partly elucidate the micro-scale mechanisms and structure of MICP and the response of hydraulic conductivities. Understanding these mechanisms might help design strategies to counter underground leakage issues. Foundation reinforcement and pollutant removal might be the areas that can also benefit from our findings. However, this study was carried out in a laboratory with ideal conditions of temperature, pH, and nutrient supply. The actual environment in the porous media is much more complex, and there are still issues that need to be solved before this technique can be widely applied.

Acknowledgements: Authors would like to thank the Ministry of Water Resources of China (201401083, 201401058, and TG1527), Nanjing Hydraulic Research Institute (Y115012), National Key R&D Plan (2016YFC0402800), and the National Science Foundation of China (41472233) for support.

REFERENCES

1. Kalkani EC (1997) Geological conditions, seepage grouting, and evaluation of piezometer measurements in the abutments of an earth dam. *Eng Geol* **46**, 93–104.
2. Singh RK, Datta M, Nema AK (2009) A new system for groundwater contamination hazard rating of landfills. *J Environ Manag* **91**, 344–57.
3. Eryürük K, Yang S, Suzuki D, Sakaguchi I, Akatsuka T, Tsuchiya T (2015) Reducing hydraulic conductivity of porous media using $CaCO_3$ precipitation induced by *Sporosarcina pasteurii*. *J Biosci Bioeng* **119**, 331–6.
4. Chu J, Stabnikov V, Ivanov V (2012) Microbially induced calcium carbonate precipitation on surface or in the bulk of soil. *Geomicrobiol J* **29**, 544–9.
5. Muynck WD, Belie ND, Verstraete W (2010) Microbial carbonate precipitation in construction materials: A review. *Ecol Eng* **36**, 118–36.
6. Burbank MB, Weaver TJ, Green TL, Williams BC, Crawford RL (2011) Precipitation of calcite by indigenous microorganisms to strengthen liquefiable soils. *Geomicrobiol J* **28**, 301–12.
7. Bachmeier KL, Williams AE, Warmington JR, Bang SS (2002) Urease activity in microbiologically-induced calcite precipitation. *J Biotechnol* **93**, 171–81.
8. Benini S, Ciurli S, Nolting HF, Mangani S (1996) X-ray absorption spectroscopy study of native and phenylphosphorodiamidate-inhibited *Bacillus pasteurii* urease. *Eur J Biochem* **239**, 61–6.
9. Benini S, Kosikowska P, Cianci M, Mazzei L, Gonzalez Vara A, Berlicki A, Ciurli S (2013) The crystal structure of *Sporosarcina pasteurii* urease in a complex with citrate provides new hints for inhibitor design. *J Biol Inorg Chem* **18**, 391–9.
10. DeJong JT, Fritzges MB, Nüsslein K (2006) Microbially induced cementation to control sand response to undrained shear. *J Geotech Geoenviron Eng* **132**, 1381–92.
11. Ferris FG, Phoenix V, Fujita Y, Smith RW (2004) Kinetics of calcite precipitation induced by ureolytic bacteria at 10 to 20 °C in artificial groundwater. *Geochim Cosmochim Acta* **68**, 1701–10.
12. Al-Thawadi S (2013) Consolidation of sand particles by aggregates of calcite nanoparticles synthesized

by ureolytic bacteria under non-sterile conditions. *J Chem Sci Tech* **2**, 141–6.
13. Chaturvedi S, Chandra R, Rai V (2006) Isolation and characterization of *Phragmites australis* (L.) rhizosphere bacteria from contaminated site for bioremediation of colored distillery effluent. *Ecol Eng* **27**, 202–7.
14. Warren LA, Maurice PA, Parmar N, Ferris FG (2001) Microbially mediated calcium carbonate precipitation: implications for interpreting calcite precipitation and for solid-phase capture of inorganic contaminants. *Geomicrobiol J* **18**, 93–115.
15. Fujita Y, Redden GD, Ingram JC, Cortez MM, Ferris FG, Smith RW (2004) Strontium incorporation into calcite generated by bacterial ureolysis. *Geochim Cosmochim Acta* **68**, 3261–70.
16. Bielefeldt AR, Illangasekare T, LaPlante R (2004) Bioclogging of sand due to biodegradation of aircraft deicing fluid. *J Environ Eng* **130**, 1147–53.
17. Mozley PS, Davis JM (2005) Internal structure and mode of growth of elongate calcite concretions: Evidence for small-scale microbially induced, chemical heterogeneity in groundwater. *Geol Soc Am Bull* **117**, 1400–12.
18. Fauriel S, Laloui L (2012) A bio-chemo-hydro-mechanical model for microbially induced calcite precipitation in soils. *Comput Geotech* **46**, 104–20.
19. Abdel Aal GZ, Atekwana EA, Atekwana EA (2010) Effect of bioclogging in porous media on complex conductivity signatures. *J Geophys Res Biogeosci* **115**, G00G07.
20. Bielefeldt AR, McEachern C, Illangasekare T (2002) Hydrodynamic changes in sand due to biogrowth on naphthalene and decane. *J Environ Eng* **128**, 51–9.
21. Fuchs S, Hahn HH, Roddewig J, Schwarz M, Turkovic R (2004) Biodegradation and bioclogging in the unsaturated porous soil beneath sewer leaks. *Acta Hydrochim Hydrobiol* **32**, 277–86.
22. Parks SL (2009) Kinetics of calcite precipitation by ureolytic bacteria under aerobic and anaerobic conditions. MSc thesis, Montana State Univ.